ELSEVIER

Chemical Engineering Journal 140 (2008) 86–100

Chemical Engineering Journal

www.elsevier.com/locate/cej

Population Balance Model (PBM) for flocculation process: Simulation and experimental studies of palm oil mill effluent (POME) pretreatment

A.L. Ahmad *, M.F. Chong, S. Bhatia

School of Chemical Engineering, Engineering Campus, Universiti Sains Malaysia, Seri Ampangan, 14300 Nibong Tebal, Penang, Malaysia

Received 6 September 2006; received in revised form 3 September 2007; accepted 10 September 2007

Abstract

The present study is intended for the first time to completely replace the inorganic coagulants with organic polymers in palm oil mill effluent (POME) pretreatment by using direct flocculation of single and dual polymer systems under applied shear. The efficiency of direct flocculation of POME was investigated by using the Population Balance Model (PBM) which considered the charge neutralization and bridging attraction under applied shear. The collision efficiency was calculated based on the Derjaguin Landau Verwey Overbeek (DLVO) theory which considered the effect of adsorbed polymer layers on van der Waals attraction and bridging attraction. This is the first attempt to correlate the floc size distribution from PBM to the indirect indicators of COD, suspended solids, oil and grease. The model predictions are in close agreement with the experimental results for both single and dual polymer systems. The interaction energy curves based on PBM shows that the flocculation using cationic polymer is by charge neutralization and bridging attraction whereas flocculation using anionic polymer is by only bridging attraction. At the optimum flocculation conditions, 99.66%, 55.79%, 99.74% and 80.78% of suspended solids, COD, oil and grease removal and water recovery are achieved, respectively. The direct flocculation process significantly reduced the treatment cost by a factor of 3.6 compared to the conventional coagulation–flocculation process.

Keywords: POME; Flocculation; Population balance modeling; Charge neutralization; Bridging attraction

1. Introduction

The production of palm oil results in the generation of large quantities of polluted wastewater referred as palm oil mill effluent (POME). A physical–chemical treatment of POME using coagulation–flocculation treatment with membrane separation could offer improved and sustainable effluent treatment [1,2]. However, in order to ensure the success of membrane separation, proper pretreatment of coagulation–flocculation process is required to reduce the suspended solids content to an acceptable level. The coagulation–flocculation process is used to mitigate membranes fouling and degradation due to suspended solids loading during the operation and thus the membrane lifespan is prolonged [2].

The most common coagulants used are hydrolysable metal cations such as lime, alum, ferric chloride and ferrous sulphate whereas polymers and polyelectrolytes are employed as flocculants. These coagulants and flocculants are not only employed in POME treatment but they are used extensively in water and wastewater treatment [3–5]. Although inorganic coagulants are inexpensive and readily available, their usage requires high chemical cost due to high dosage. It also generates excessive volumes of phyto-toxic sludge and cannot be readily disposed. A large amount of caustic is needed to alter the solution pH to achieve its isoelectric point and coupling with flocculation is needed to improve the efficiency [6].

The polyelectrolytes of organic macromolecules polymers offer significant advantages in coagulation–flocculation process. The concentrations needed are only a few milligrams per liter and they generate small quantity of non-hazardous sludge for easy disposal. On a price-per-weight basis, they are much more expensive than inorganic coagulants, but overall operating cost is lower because of a reduced dosage, elimination of pH adjusting

* Corresponding author.
E-mail address: chlatif@eng.usm.my (A.L. Ahmad).

1385-8947/$ – see front matter © 2007 Elsevier B.V. All rights reserved.
doi:10.1016/j.cej.2007.09.014

Nomenclature

a_m	effective monomer size (nm)
A_p, A_m, A_s	Hamaker constant of the solids, solvent and polymer, respectively (J)
b_R	fitting parameter in Eq. (10), dimensionless
b_1	constant in Eq. (16), dimensionless
b_2	constant in Eq. (18), dimensionless
C_L	aggregate structure prefactor, dimensionless
$C_{O\&G}$	oil and grease concentration (mg/L)
C_{SS}	suspended solids concentration (mg/L)
$COD_{soluble}$	soluble COD (mg/L)
COD_{total}	total COD (mg/L)
d_{am}	arithmetic mean floc diameter (μm)
d_F	fractal dimension, dimensionless
$\bar{d}_i$	arithmetic mean diameter of flocs in size class i (μm)
D	impeller diameter (m)
D_{sc}	scaling length (nm)
e	elementary charge (C)
E_f	fluid collection efficiency of an aggregate, dimensionless
G	global average fluid velocity gradient or shear rate (s^{-1})
h_0	minimum separation distance between particle surfaces (nm)
$H_{(x,y)}$	unretarded geometric functions, dimensionless
K	Debye-Hückel parameter (J/m^3C)
K_B	Boltzmann constant (J/K)
m_i	salt concentration (mol/m^3)
n	number concentration of particles or aggregates (m^{-3})
N	rotational speed (rpm)
N_{AV}	Avogadro's number (mol^{-1})
N_i	number concentration of particles or aggregates in section i (m^{-3})
N_P	power number of impeller (W)
$\bar{r}$	mass mean aggregate radius (μm)
r_{ci}, r_{cj}	floc collision radius (μm)
r_i	particle radius at size class i (μm)
r_{0i}, r_{0j}	primary particles radii (μm)
r_0	composite radius of a particle with adsorbed polymer layers (μm)
s	distance between particles centers (nm)
S	specific rate constant of fragmentation (s^{-1})
t	flocculation time (s)
T	suspension temperature (K)
v, u	particle or aggregate volumes (m^3)
V	volume of the suspension (J)
V_{edl}	electrical double layer repulsion (J)
V_T	net interaction energy between two primary particles (J)
V_s	energy of steric repulsion or bridging attraction (J)
V_{vdw}	Van der Waals energy (J)
z_c	valence of counterion, dimensionless
z_i	valence of electrolyte ions, dimensionless

Greek letters

α	collision efficiency factor, dimensionless
α_{Sc}	numerical constant, dimensionless
β	collision frequency factor (m^3/s)
γ	breakage distribution function, dimensionless
Γ	total amount of polymer adsorbed on a single surface
Γ_0	adsorbed amount at saturation
δ	adsorbed polymer layer thickness (nm)
$\bar{\varepsilon}$	average turbulent energy dissipation rate (m^2/s^3)
ε_0, ε_r	dielectric constant of a vacuum and the solvent (C/mV)
λ_R	characteristic wavelength of interaction (nm)
μ	fluid dynamic viscosity (kg/ms)
υ	kinematic viscosity (m^2/s)
ρ	density of the suspension (kg/m^3)
ρ_p	particle density (kg/m^3)
υ_i	floc volume fraction in size class i, dimensionless
ψ_{0i}, ψ_{0j}	surface potential (mV)
Φ_{so}	polymer volume fraction at a single saturated surface, dimensionless

chemicals and reduced sludge disposal costs due to lower sludge volumes [7].

The objective of current work is to completely replace the inorganic coagulants with water-soluble organic polyelectrolytes/polymers in POME pretreatment by using direct flocculation (i.e. without addition of coagulants) under a constant applied shear. The flocculation process investigated in the present study is the single and dual polymer systems. The single polymer system utilizes the medium charge density with high molecular weight cationic polymer. The cationic polymer served as double acting polymer by first neutralizing the negative charge of the particles (charge neutralization) and then visible flocs formation by bridging. The dual polymer system is employed when the single polymer system failed to achieve the desired flocculation. In this system, the cationic polymer is first added for charge neutralization and bridging. The bridging-type long chain anionic polymer is then added to further enhance the bridging effects by mechanically bridging the flocs into larger and rapid settling flocs (dense flocs).

The polymer-induced flocculation efficiency is commonly evaluated by water recovery, suspended solids, COD, oil and grease removal. However, these are only indirect indicators of the effectiveness of flocculation. These indirect indicators are unable to ascertain the dominant mechanism of flocculation of whether it is charge neutralization, bridging or both. The most explicit and direct measure of flocculation efficiency is floc size distribution. The Population Balance Modeling (PBM) has been used extensively to simulate the evolution of floc size distribution with time to investigate the efficiency of the flocculation process [8–13].

Somasundaran and Runkana [8] proposed a complete flocculation model for colloidal mineral suspensions using the PBM.

The influence of surface forces in the presence of salts and polymers was incorporated into the PBM to obtain an analytical solution for the collision efficiency. The collision efficiency is an important parameter in PBM and it is previously employed as a fitting parameter. Runkana et al. [9,10] also proposed a mathematical model based on PBM for processes involving polymer-induced flocculation via simple charge neutralization using the modified Derjaguin Landau Verwey Overbeek (DLVO) theory. The effect of adsorbed polymer layers on van der Waals attraction was included. The investigation was also extended by considering the effects of bridging attraction or steric repulsion due to the adsorbed polymer layers based on scaling theory.

However, the PBM for polymer-induced flocculation by charge neutralization and bridging attraction presented in the literature focused on perikinetic aggregation of Brownian motion and differential sedimentation. Orthokinetic aggregation due to applied shear is commonly applied to accelerate the flocculation process. Therefore, the PBM suitable for polymer-induced flocculation by charge neutralization and bridging under applied shear is proposed in the present study to investigate the efficiency of the flocculation process in POME pretreatment. Besides, the current investigation attempt for the first time to correlate the information of floc size distribution from the PBM to the indirect indicators of COD, suspended solids, oil and grease. In addition, a preliminary cost analysis is also carried out to evaluate and compare the treatment costs between the direct flocculation and the conventional coagulation–flocculation process.

2. Model development

Population Balance Model (PBM) of Smoluchowski [14] is the most informative for modeling aggregation phenomena in colloidal suspensions. In the aggregation–fragmentation processes, fragmentation is generally assumed to take place only due to fluid stress and not due to collisions between different aggregates, though it is also possible. The incorporation of both aggregation and fragmentation kinetics in the PBM is given by the following partial integra-differential equation [15]:

$$\frac{\partial n(v,t)}{\partial t} = -\int_0^\infty \alpha(v,u)\beta(v,u)n(v,t)n(u,t)\mathrm{d}u + \frac{1}{2}\int_0^v \alpha(v-u,u)\beta(v-u,u)n(v-u,t)n(u,t)\mathrm{d}u - S(v)n(v,t) + \int_v^\infty S(u)\gamma(v,u)\mathrm{d}u \quad (1)$$

where n is the number concentration of particles or aggregates, v and u the particle or aggregate volumes, t the flocculation time, α the collision efficiency factor, β the collision frequency factor, S the specific rate constant of fragmentation and γ is breakage distribution function. The first term in the Eq. (1) accounts for loss or disappearance of particles or aggregates of size v due to their interaction with primary particles or aggregates belonging to all size classes. The second term represents the growth of aggregates due to the interaction between primary particles and aggregates belonging to smaller size classes. The third term accounts for the loss of aggregation due to fragmentation while the last term represents generation of primary particles or smaller aggregates due to breakage or erosion of larger aggregates.

Eq. (1) is a stochastic model. It is necessary to employ numerical solution after discretizing the equation with respect to size into a set of nonlinear ordinary differential equation (ODE). Based on the geometric discretization techniques [16], the rate of change of particle or aggregate number concentration during the simultaneous aggregation and fragmentation is given by the following discretized and lumped PBM:

$$\frac{\mathrm{d}N_i}{\mathrm{d}t} = \frac{1}{2}\alpha_{i-1,i-1}\beta_{i-1,i-1}N_{i-1}^2 + N_{i-1}\sum_{j=1}^{i-2}2^{j-i+1}\alpha_{i-1,j}\beta_{i-1,j}N_j - N_i\sum_{j=1}^{i-1}2^{j-i}\alpha_{i,j}\beta_{i,j}N_j - N_i\sum_{j=i}^{\max_1}\alpha_{i,j}\beta_{i,j}N_j - S_iN_i + \sum_{j=i}^{\max_2}\gamma_{i,j}S_jN_j \quad (2)$$

where N_i is the number concentration of particles or aggregates in section i, $\max_1$ is maximum number of sections used to represent the complete aggregate size spectrum and $\max_2$ corresponds to the largest section from which flocs in the current section are produced by fragmentation. The first and second terms on the right of Eq. (2) account for growth, while the third and fourth terms account for loss of aggregates by aggregation, fifth term accounts for the loss of aggregates due to fragmentation and the last term account for generation of smaller aggregates due to breakage or erosion. The flocculation can be visualized as a three-step process: aggregate transport represented by the collision frequency factor, $\beta_{i,j}$, attachment given by the collision efficiency, $\alpha_{i,j}$ and aggregates breakage represented by the specific rate constant of fragmentation, S_i and breakage distribution function $\gamma_{i,j}$.

2.1. Collision frequency

In the wastewater treatment system, orthokinetic aggregation (aggregation due to applied shear) is often preferred. In the pretreatment of POME, shear is applied by the stirring motion of impeller to accelerate aggregation process and therefore, the gravitational contribution is being neglected. The collision frequency factor of orthokinetic [8] is given by

$$\beta_{i,j}^{\mathrm{sh}} = \frac{4}{3}G\left(\sqrt{E_{\mathrm{f}i}}r_{ci} + \sqrt{E_{\mathrm{f}j}}r_{cj}\right)^3 \quad (3)$$

where G is the global average fluid velocity gradient or shear rate, r_{ci} or r_{cj} the floc collision radius, and E_{f} is the fluid collection efficiency of an aggregate. The E_{f} is in the range of $0 \le E_{\mathrm{f}} \le 1$. The collision frequency factor for permeable aggregates can be reverted to those for rigid spheres (rectilinear model) by setting E_{f} equal to 1. If the E_{f} is less than 1, it is curvilinear model

[17,18]. The shear rate, G can be obtained as [19]

$$G = \sqrt{\frac{N_P \rho N^3 D^5}{V\mu}} = \sqrt{\frac{\bar{\varepsilon}}{v}} \tag{4}$$

where N_P is the power number of impeller, ρ the density of the suspension, N the rotational speed, D the impeller diameter, V the volume of the suspension, μ the fluid dynamic viscosity, $\bar{\varepsilon}$ the average turbulent energy dissipation rate and v is the kinematic viscosity. The flocs collision radius of an aggregate, r_{ci} containing n_0 primary particles is given by [20]

$$r_{ci} = r_0 \left(\frac{n_{0i}}{C_L}\right)^{1/d_F} \tag{5}$$

where C_L is the aggregate structure prefactor, r_0 is the composite radius of a particle with adsorbed polymer layers and d_F is the fractal dimension. The collision frequency of Eq. (3) can be computed by assigning appropriate values of d_F. The fractal dimension is an indirect indicator of the flocs structure and its openness. The fractal dimension is used to incorporate the qualitatively analysis of flocs structure into the PBM which is quantitative (number and radii of flocs).

2.2. Collision efficiency

The collision efficiency factor is computed as the reciprocal of the Fuchs' stability ratio, W between the primary particles [8]

$$W_{i,j} = (r_{0i} + r_{0j}) \int_{r_{0i}+r_{0j}}^{\infty} \frac{\exp(V_T/K_B T)}{s^2} ds \tag{6}$$

where V_T is net interaction energy between two primary particles of radii r_{0i} and r_{0j}, s the distance between particles centers ($s = r_{0i} + r_{0j} + h_0$), h_0 the minimum separation distance between particle surfaces, K_B is the Boltzmann constant and T is the suspension temperature.

In the Derjaguin Landau Verwey Overbeek (DLVO) theory [8–10], the net interaction energy between two primary particles, V_T is equal to the sum of Van der Waals energy, V_{vdw}, electrical double layer repulsion, V_{edl} and energy of steric repulsion or bridging attraction, V_s

$$V_T = V_{vdw} + V_{edl} + V_s \tag{7}$$

2.2.1. Van der Waals energy

In the case where inorganic coagulant is used as the coagulant, the Van der Waals energy of attraction between bare particles, V_{vdw}^H should be considered [8].

$$V_{vdw}^H = -\frac{A}{6}\left\{\frac{2r_{0i}r_{0j}}{s^2 - (r_{0i} + r_{0j})^2} + \frac{2r_{0i}r_{0j}}{s^2 - (r_{0i} - r_{0j})^2} + \ln\left[\frac{s^2 - (r_{0i} + r_{0j})^2}{s^2 - (r_{0i} - r_{0j})^2}\right]\right\} \tag{8}$$

where A is the Hamaker constant of solids across the solvent medium. However, in the case where polymer is used, the adsorbed polymer layers on the particles should be considered. The expression for the Van der Waals energy for the case of two solids of the same kind with equal adsorbed polymer layer thickness is [8,21,22]

$$\begin{aligned} -12V_{vdw}^V = {} & H_{sisj}(A_{si}^{1/2} - A_m^{1/2})(A_{sj}^{1/2} - A_m^{1/2}) \\ & + H_{pipj}(A_{pi}^{1/2} - A_{si}^{1/2})(A_{pj}^{1/2} - A_{sj}^{1/2}) \\ & + H_{pisj}(A_{pi}^{1/2} - A_{si}^{1/2})(A_{sj}^{1/2} - A_m^{1/2}) \\ & + H_{pjsi}(A_{pj}^{1/2} - A_{sj}^{1/2})(A_{si}^{1/2} - A_m^{1/2}) \end{aligned} \tag{9}$$

where A_p, A_m and A_s are the Hamaker constant of the solids, solvent and polymer, respectively across vacuum, $H_{(x,y)}$ is the unretarded geometric functions. The retardation effect is incorporated by multiplying the unretarded Van der Waals energy between the polyelectrolyte-coated particles with a correction function, $f_{R(h_0)}$ [23].

$$f_{R(h_0)} = 1 - \frac{b_R h_0}{\lambda_R} \ln\left(1 + \frac{\lambda_R}{b_R h_0}\right) \tag{10}$$

λ_R is the characteristic wavelength of interaction, 100 nm and b_R is a fitting parameter of 5.32.

2.2.2. Electrical double layer repulsion

The interaction energy due to the electrical double layers between two spheres of radii, (r_{0i} and r_{0j}) and surface potentials, ψ_{0i} and ψ_{0j} is given by [24]

$$V_{edl} = 64\pi\varepsilon_0\varepsilon_r \left(\frac{K_B T}{z_c e}\right)^2 \left(\frac{r_{0i}r_{0j}}{r_{0i} + r_{0j}}\right) \tanh\left(\frac{z_c e\psi_{0i}}{4K_B T}\right) \times \tanh\left(\frac{z_c e\psi_{0j}}{4K_B T}\right) \exp(-Kh_0) \tag{11}$$

where e is the elementary charge, z_c is the valence of counter ion, ε_0, ε_r are the dielectric constant of vacuum and the solvent and K is the Debye-Hückel parameter which is defined as [25]

$$K = \frac{N_{AV} e^2 \sum_i m_i z_i^2}{\varepsilon_0 \varepsilon_r K_B T} \tag{12}$$

where N_{AV} is the Avogadro's number, m_i is salt concentration and z_i is valence of electrolyte ions. The i in Eq. (12) refers to an electrolyte species in solution.

2.2.3. Bridging attraction

The interaction energy due to bridging attraction (V_s) is dependant on the adsorbed polymer layers. It is important to understand the electrochemical changes brought by the adsorbed polymer on particle surfaces. The scaling theory [26,27] is used to compute forces due to adsorbed polymer layers. It was chosen because it permits derivation of analytical formulas for interaction between spherical particles. The scaling theory is based on minimization of a surface free energy functional subject to the constraint that total amount of polymer adsorbed is fixed in the region between two surfaces having adsorbed layers. The interaction energy due to bridging attraction between two unequal

polymer-coated spheres can be computed as [9]

$$V_s = \left(\frac{2\pi r_{0i} r_{0j}}{r_{0i} + r_{0j}}\right)\left(\frac{\alpha_{Sc} K_B T}{a_m^3}\right)\Phi_{so}^{9/4} D_{Sc}\left\{-\frac{16\Gamma D_{Sc}}{\Gamma_0} \times \ln\left(\frac{2\delta}{h_0}\right) + \frac{4D_{Sc}^{5/4}}{2^{5/4}}\left(\frac{8\Gamma}{\Gamma_0}\right)^{9/4}\left[\frac{1}{h_0^{1/4}} - \frac{1}{(2\delta)^{1/4}}\right]\right\} \quad (13)$$

where δ is the adsorbed polymer layer thickness, α_{Sc} is numerical constant which can be obtained from osmotic pressure and light scattering experiments on polymer solution, a_m is effective monomer size, Γ is total amount of polymer adsorbed on a single surface, D_{Sc} is the scaling length, Φ_{so} is polymer concentration at a single saturated surface and Γ_0 is adsorbed amount at saturation.

The proposed scaling theory of Eq. (13) is based on flocculation in the absence of shear. When shear is applied, there will be lateral sliding and friction forces besides the normal forces. Due to the lateral shear stress, the adsorbed polymer chains may swell or stretch because of the fluid velocity gradients and osmotic pressure can increase as the fluid tries to squeeze out of the gap between particle surfaces. The chain may get desorbed if the shear rate is too high. However, shear forces between surfaces covered with adsorbed polymers have not been studied, either theoretically or experimentally [9]. Due to current limitations, the scaling theory is being applied in the modeling of flocculation under applied shear by ignoring the sliding and friction forces on the adsorbed layer.

2.3. Aggregates breakage

The increase of collision frequency by applying shear does not necessary result in high rates of flocculation. Aggregates breakage or fragmentation often occurs due to shear stress especially at high stirring speed. The parameters used to compute the aggregates breakage is the specific rate constant of fragmentation, S_i and the breakage distribution function, $\gamma_{i,j}$. The specific rate constant of fragmentation, S_i is defined as [8,28]

$$S_i = \left(\frac{4}{15\pi}\right)^{1/2}\left(\frac{\bar{\varepsilon}}{v}\right)^{1/2}\exp\left(\frac{-\varepsilon_{b,i}}{\bar{\varepsilon}}\right) \quad (14)$$

where $\varepsilon_{b,i}$ is the critical turbulent energy dissipation rates at which floc breakage takes place. The breakage distribution function, $\gamma_{i,j}$ is a fitting parameter.

2.4. Dynamic scaling

As aggregation proceeds, flocs developed as porous object with highly irregular and open structures. PBM represent aggregation process quantitatively (number and radii of flocs), however it does not compute the aggregates quality in terms of flocs compactness. Flocs quality besides having large aggregate radii, compactness of the flocs is also crucial to assist sedimentation and liquid–solid separation. The fractal dimension, d_F is a simple parameter to represent the complex structure of aggregates. The fractal dimension fall in the range of $1 \leq d_F \leq 3$ [29]. The formed aggregates are more compact when the system has high fractal dimension. The fractal dimension of polymer flocculated flocs ranges from 1.7 to 2.5 [18]. The fractal dimension can be computed by using the scaling-law for mean aggregate size as a function of time [30]:

$$\bar{r} \propto t^{1/d_F} \quad (15)$$

where $\bar{r}$ is the mass mean aggregate radius. A plot of $\log(\bar{r})$ against $\log(t)$ will be a straight line and d_F can be obtained as the reciprocal of the slope.

3. Materials and methods

3.1. Materials

Raw POME was collected from United Palm Oil Mill, Sungai Kecil Nibong Tebal, Penang, Malaysia and stored in cool room at 4 °C. The cationic polymer used was the medium charge density with high molecular weight (Polyfloc KP 9650) while the anionic polymer used was the high charge density with high molecular weight (Polyfloc AP 8350). Both polymers were provided by Hexagon Chemical. In all experimental tests, the appropriate mass of cationic and anionic polymer was dissolved in water to give 0.1%, w/v and 0.2%, w/v feedstock solution, respectively. These feedstock solution concentrations were recommended by their manufacturers in order to ensure the optimum performance of the polymers.

3.2. Jar test procedure

Experiments were carried out in a jar test apparatus (Flocculator SW1, Stuart Scientific, UK) equipped with six beakers of 1 L volume. Raw POME sample was thawed to room temperature. The sample was shaken thoroughly for re-suspension of possible settled solids and analyzed with respect to its initial suspended solids, COD, soluble COD, oil and grease. The sample was transferred into the 400 mL beakers. The appropriate dosage of cationic and anionic polymers was added into the samples while stirring at 200 rpm and 150 rpm, respectively for 1–6 min. The sample was left to settle for 1 min and the sample from the supernatant was taken and analyzed with respect to the concentration of suspended solids, COD, soluble COD, oil and grease. The parameters of suspended solids, COD, soluble COD, oil and grease were analyzed using procedures outlined in the standard methods [31]. The water recovery was measured by collecting all the filtered supernatant in a graduated cylinder from the supernatant–sludge mixture through a belt cloth with the pores of 500 μm.

3.3. Dynamic light scattering

Dynamic light scattering was employed to determine the time evolution of the aggregate/floc size distribution. Experiments were conducted using the jar test apparatus. Four hundred millilitres of raw POME was stirred in the jar test apparatus which can stir six beakers simultaneously at the exact same shear rate. The polymer was added into each beaker at exact same dosage,

Table 1
Characteristic of palm oil mill effluent (POME)

Parameter	Value
pH	4.1
Total COD (mg/L)	38,000
Soluble COD (mg/L)	18,000
Suspended solids (mg/L)	14,800
Oil and grease (mg/L)	3700
Potassium (mol/m^3)	58
Magnesium (mol/m^3)	25
Calcium (mol/m^3)	10
Particle concentration (no./m^3)	2.334×10^{11}
Primary particle mean diameter (μm)	64.2
Particle density (kg/m^3)	600
Suspension Density (kg/m^3)	1000
Temperature (K)	298
Viscosity (Pa s)	1.0240×10^{-3}

the reaction time was measured. The floc size distribution was measured by pumping the solution into the measurement cell of a laser granulometer (Mastersizer, Malvern) using a peristaltic pump. The pump is placed after the measurement cell. The light scattering data are recorded while the solution flowed into the measurement cell. As the solution was discarded after measurement, each beaker corresponded to a particular time in the aggregation kinetics. The experiments were repeated at varying polymer dosage.

4. Results and discussion

Prior to the implementation of the PBM and the analysis of flocculation efficiency, understanding the characteristic and the behavior of the initial flocculating suspension (raw POME) is very important. Based on the characteristic of the raw POME as listed in Table 1, the insoluble COD constitutes more than half of the total COD and is closely related to the concentration of suspended solids. By assuming that the insoluble COD is solely contributed by the suspended solids (C_{SS}), the suspended solids can be correlated to the total COD (COD_{total}) of the suspension as

$$COD_{total} = b_1 C_{SS} + COD_{soluble} \quad (16)$$

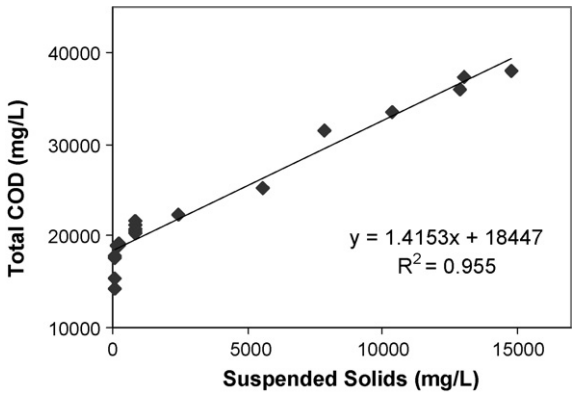

Fig. 1. Linear plot of total COD against the suspended solids concentration.

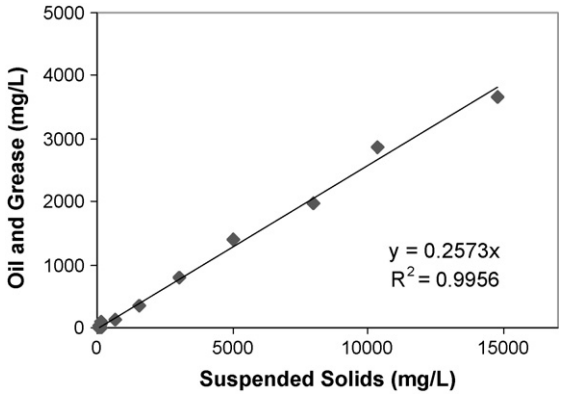

Fig. 2. Linear plot of oil and grease concentration against the suspended solids concentration.

A linear plot of total COD against the suspended solids concentration where the intercept of y-axis indicates the value of soluble COD ($COD_{soluble}$) is shown in Fig. 1. The values of $b_1 = 1.4153$ and $COD_{soluble} = 18.447$ are obtained and the fitted soluble COD value is close to the experimental value as indicated in Table 1. Thus the final correlation is obtained as

$$COD_{total} = 1.4153 C_{SS} + 18447 \quad (17)$$

Since the un-extracted oil is contained inside the crunched fruit shell and the removal of suspended solids will simultaneously remove the oil and grease from the POME, suspended solids can also be correlated to the oil and grease concentration ($C_{O\&G}$) by using the correlation as

$$C_{O\&G} = b_2 C_{ss} \quad (18)$$

Based on Eq. (18), the linear plot of oil and grease concentration against suspended solids concentration is shown in Fig. 2 and the slope of the plot give the value of $b_2 = 0.2573$. Thus, the final correlation is obtained as

$$C_{O\&G} = 0.2573 C_{ss} \quad (19)$$

The primary particle mean diameter as shown in Table 1 is obtained based on the particle size distribution data (Fig. 3) which is measured by injecting the raw POME into the laser

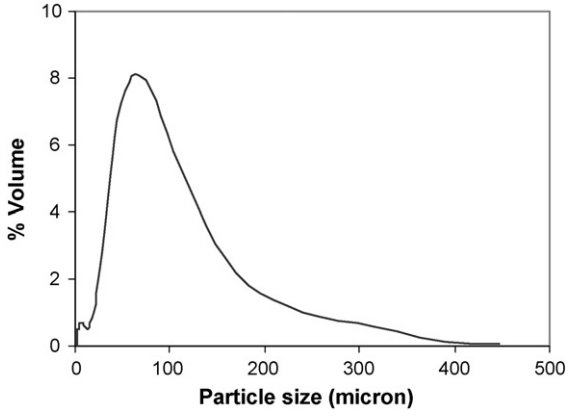

Fig. 3. Particle size distribution data for raw POME.

granulometer (Mastersizer, Malvern). The particle size distribution of raw POME in Fig. 3 shows that the particles of raw POME are polydisperse with varying particle size ranging from 1.4 to 450 μm and these particles are measured as suspended solids. For the sake of simplicity, during the implementation of the PBM, the raw POME is considered as monodisperse system by using its mean diameter. However, for the calculated particle concentration for each size class (N_i) which is less than 450 μm, these are summed as the suspended solids through the particle density (ρ_p) by assuming that particles remained as the fine particles which are not being flocculated into flocs large enough for separation.

$$C_{SS} = \rho_p \sum_{i=1}^{k} \frac{4}{3}\pi r_i^3 N_i \tag{20}$$

where r_i is the particle radius at size class i and k is the size class at which the particle size is less than 450 μm. Based on Eqs. (16)–(20), the correlation between the indirect indicators (suspended solids, COD, oil and grease) and the PBM is obtained. It must be noted that POME is a complex system with the mixture of suspended solids, oil and grease as well as other soluble organic components. The PBM can be used to represent the flocculation process of POME system in the present study by assuming only suspended solids which contributing to the insoluble COD, oil and grease are removed as flocs. This assumption is valid because the concentration of soluble organic components in POME represented by the soluble COD remains unchanged before and after flocculation.

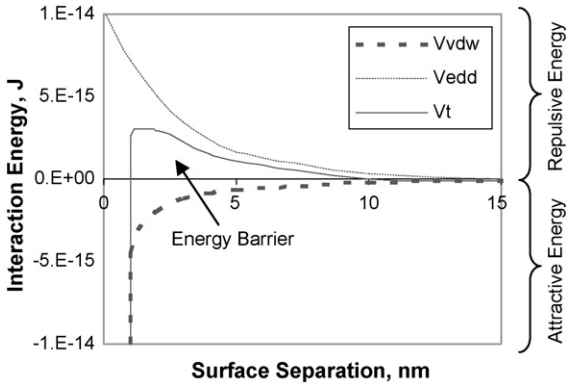

Fig. 4. The interaction energy curves for bare particles of raw POME. V_{vdw} is van der Waals attraction, V_{edd} is electrical double layer repulsion and V_t is the net interaction energy.

The kinetics of aggregation and the size of aggregates are highly depended on the initial flocculating suspension. The particle surface chemistry influences the probability of attachment between colliding particles and strength of resulting aggregate. In most colloidal systems, this is due to the van der Waals attraction and electrical repulsion forces which are the basis of the DLVO theory. There are also other non-DLVO forces such as the hydration effects, as well as hydrophobic and steric interactions that may play crucial roles in certain processes [32].

In the present investigation, the initial flocculating suspension (raw POME) is tested against the forces of van der Waals attraction and electrical repulsion from the basis of DLVO theory based on Eqs. (8) and (11). According to DLVO theory, the

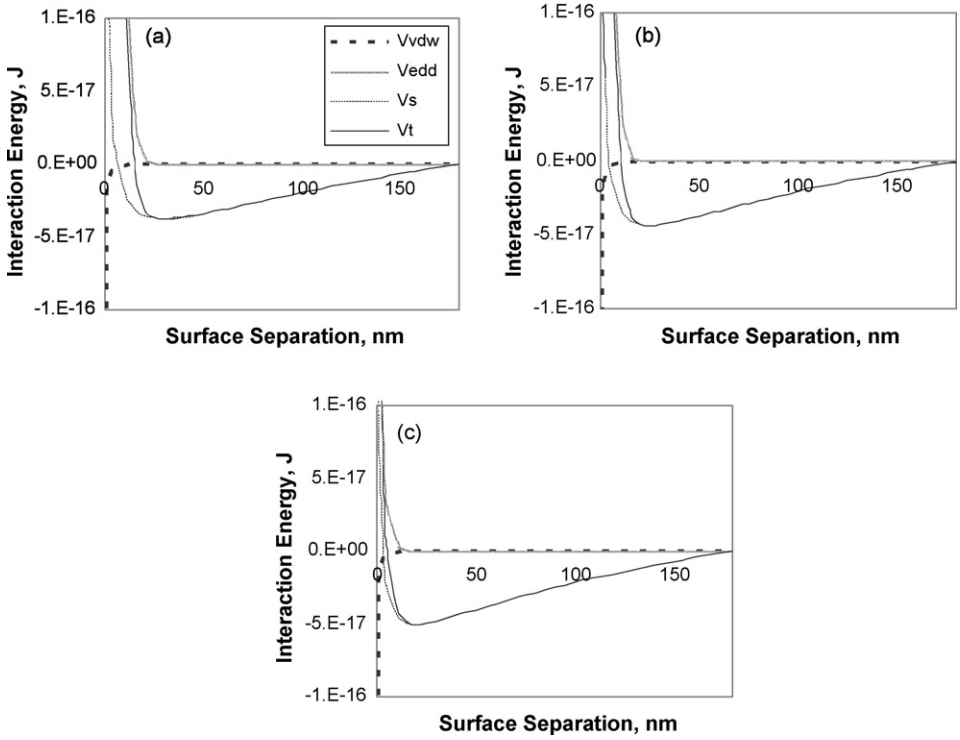

Fig. 5. The interaction energy curves for particles of POME with adsorbed cationic polymer layers at the dosage of (a) 100 ppm with Γ/Γ_0 0.600, ψ_0 −87.2 mV; (b) 200 ppm with Γ/Γ_0 0.625, ψ_o −32.6 mV; (c) 300 ppm with Γ/Γ_0 0.650, ψ_0 12.5 mV. V_{vdw} is van der Waals attraction, V_{edd} is electrical double layer repulsion, V_s is bridging attraction and V_t is the net interaction energy.

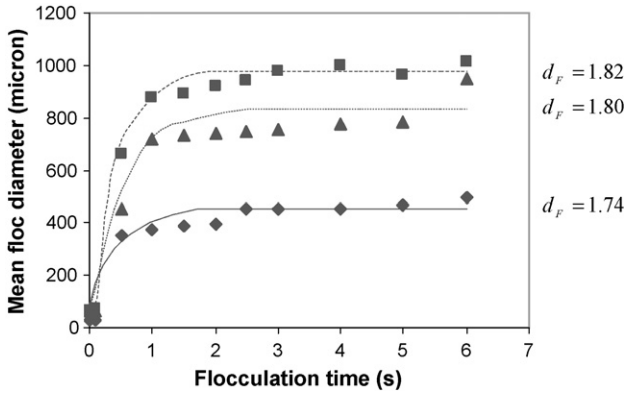

Fig. 6. Comparison of simulated and experimental time evolution of mean floc diameter with different cationic polymer dosage. Experimental: (♦) 100 mg/L, (▲) 200 mg/L, (■) 300 mg/L and simulation: (——) 100 mg/L, (. . .) 200 mg/L, (—) −300 mg/L.

primary net interaction energy between the bare particles of raw POME is equal to the sum of van der Waals attraction and electrical repulsion between the particles. Fig. 4 shows the interaction energy curves between the bare particles of raw POME. Based on the measured surface potential (assuming the zeta potential is close to its surface potential) of −93 mV, the net interaction energy falls in the repulsive region which is termed as the energy barrier due to the significant electrical double layer repulsion. In order for the particles to agglomerate, the energy barrier must be lowered or completely removed by effective flocculation so that the net interaction energy is always attractive [33].

4.1. Single polymer system

For the single polymer system, the direct flocculation of POME was investigated by using medium charge density with high molecular weight cationic polymer (Polyfloc KP 9650) at the dosage of 100, 200 and 300 mg/L, respectively under constant shear of 200 rpm. The raw POME was flocculated at its initial pH (without pH adjustment) and the floc size distribution data, pretreated POME suspended solid, COD, oil and grease were obtained for each reaction time of 1–6 min.

The flocculation efficiency of POME is investigated based on PBM. The discretized PBM of Eq. (2) forms a set of nonlinear ODEs and was solved numerically by the orthogonal collocation technique [34]. During the integration of the PBM equations, the calculated floc size distribution was tested for conservation of solid volume at each reaction time. The results obtained in the present investigation had the loss of total solid volume of less than 1%.

Table 2
Model parameters used in PBM for cationic polymer-induced flocculation

Parameter	Value
Boltzmann constant, K_B	1.3807×10^{-23} J/K
Avogadro's number, N_{AV}	6.022×10^{23}
Elementary charge, e	1.6×10^{-19} C
Kinematic viscosity, ν	1.0×10^{-6} m^2 s^{-1}
Hamaker constant of the solids across a vacuum, A_p	6.0×10^{-20} J*
Hamaker constant of the solvent across a vacuum, A_m	3.7×10^{-20} J
Hamaker constant of the polyacrylamide across a vacuum, A_s	8.0×10^{-20} J**
Dielectric constant of the vacuum	8.85×10^{-9} C/mV
Polymer volume fraction at a single saturated surface, Φ_{So}	0.18
Scaling length, D_{Sc}	4 nm
The term $\alpha S_c k_B T/a_m^3$ of Eq. (13)	3×10^5 N/m^2
Adsorbed polymer layer thickness, δ	90 nm
Fractional polymer surface coverage, Γ/Γ_0	0.60–0.65
Surface potentials, ψ_{0i}	−87.2–12.5 mV

*Data from Van Oss [37]; **Data from Israelachvili [25].

The PBM of Eq. (2) involves a number of parameters; which are the collision frequency factor, $\beta_{i,j}$, the collision efficiency, $\alpha_{i,j}$ and the specific rate constant of fragmentation, S_i. These parameters can be calculated theoretically by setting the breakage distribution function $\gamma_{i,j}$ as a fitting parameter once the fractal dimension is obtained based on the dynamic scaling analysis. In the case where the model parameters values were not reported or could not be obtained experimentally due to insufficient equipment, representative values were taken from literature and adjusted by trial and error to match the measured floc distribution data. The initial estimation of parameters in the Eq. (13) for interaction energy due to adsorbed polymer layers (bridging attraction) can by obtained from the literature. The initial estimation for the term $\alpha S_c k_B T/a_m^3$ of Eq. (13) is obtained as 3×10^5 N/m^2 according to Klein and Rossi [35] based on polyethylene oxide (PEO)-coated mica surfaces system. The D_{Sc} is obtained as 4 nm for the polymer volume fraction at saturation, Φ_{So} of around 0.3 as reported by Cosgrove et al. [36] based on the volume fraction profiles of PEO

Table 3
Experimental data and model parameters employed in the simulation studies

Run #	Polymer concentration (mg/L)		d_F	Water recovery	Suspended solids removal (%)	COD removal (%)	Oil and grease removal	Measured zeta potential (%)	Fitted surface potential (mV)
	Cationic	Anionic							
1	100	–	1.74	13.33	94.53	43.19	95.12	−92.4	−87.2
2	200	–	1.80	45.65	98.72	50.26	98.10	−31.0	−32.6
3	300	–	1.82	55.65	99.60	53.68	99.74	+16.8	+12.5
4	300	10	1.82	61.87	99.54	53.68	99.66	+13.5	+12.1
5	300	30	1.83	69.81	99.61	55.27	99.85	+10.7	+11.7
6	300	50	1.85	80.78	99.66	55.79	99.74	−6.2	−4.4

d_F is the aggregate fractal dimension which were obtained by dynamic scaling.

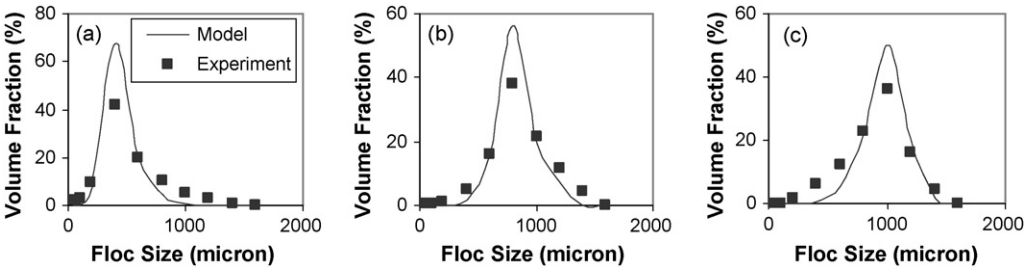

Fig. 7. Comparison of simulated and experimental floc size distribution obtained after 6 min of flocculation using (a) 100 mg/L; (b) 200 mg/L; (c) 300 mg/L cationic polymer.

on polystyrene surfaces. Although these values assigned are of different polymer–substrate system, they are assumed to be applicable to the present system. In order to check the validity of the assigned values, interaction energies for each system of different cationic polymer dosage (100, 200, 300 mg/L) were computed between two polymer-coated particles having the identical bare particle diameter of 64.2 μm. The parameters ψ_0, Φ_{So}, δ and Γ/Γ_0 were adjusted so that the net interaction energy is attractive. After some trials, the values of ψ_0, Φ_{So}, δ and Γ/Γ_0 were obtained as −87.2–12.5 mV, 0.18, 90 nm and 0.6–0.65, respectively and the detail model parameters and their values used in PBM simulation are shown in Table 2.

Based on the model parameters of Table 2, the computed interaction energy profiles at different cationic polymer dosage of 100, 200 and 300 ppm are shown in Fig. 5. By comparing the interaction energy curves of Fig. 4 against Fig. 5, the adsorbed cationic polymer layers on the particles surface had greatly lowered the surface charge-by-charge neutralization and the electrical double layer repulsion is almost zero. Thus, the energy barrier of the system is greatly lowered or eliminated. At the same time, bridging attraction is present due to the adsorbed polymer layers. Bridging is often occurred in conjunction with charge neutralization of cationic polymer to grow fast settling and shear resistant flocs [17]. It is weakly attractive at long distances and becomes progressively stronger as the particles approach closer. The particle surfaces repel each other at short distances due to the compression of the adsorbed layer. As results, the bridging attraction dominated and resulted in net attraction.

Table 3 shows the experimental data and the model parameters used in the simulation studies. The fractal dimensions of the aggregate were obtained by dynamic scaling as discussed in Eq. (15). The surface potential of particles is difficult to measure and is normally assumed approximately equal to its zeta potential. However, when particles have adsorbed polymer layers, surface potential could be quite different from zeta potential and it becomes necessary to adjust the surface potential in order to match the computed results with the experimental data. Nevertheless, fitted surface potentials turn out to be fairly close to measured zeta potentials as shown in Table 3. In order to test the model for dynamics of flocculation at a different level, simulation results using PBM are compared in Figs. 6 and 7 with

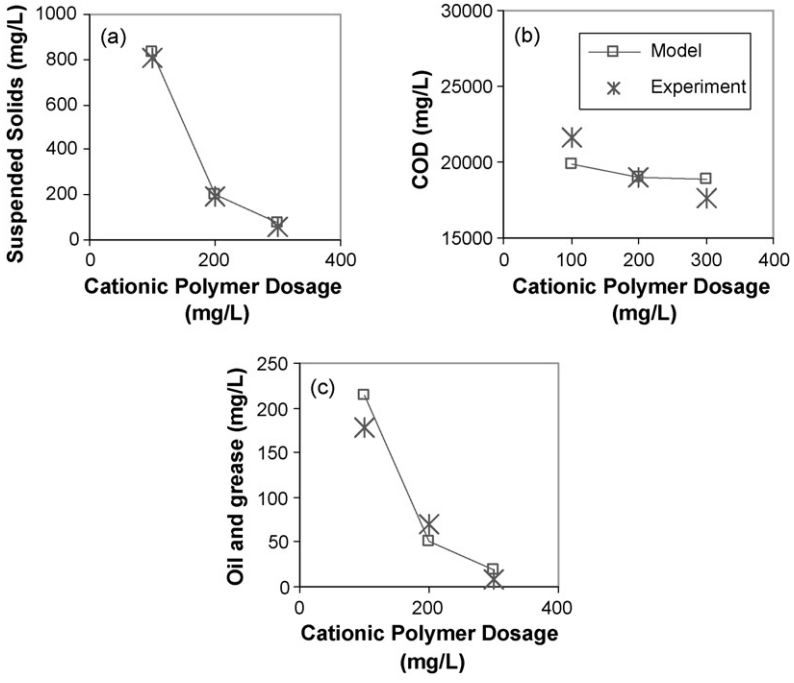

Fig. 8. Effect of cationic polymer dosage on (a) suspended solids; (b) COD; (c) oil and grease concentration of pretreated POME.

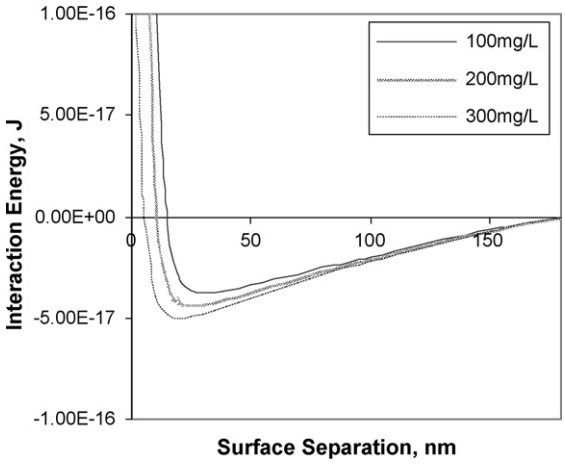

Fig. 9. Comparison of net interaction energy between different cationic polymer dosage.

experimental results for time evolution of mean floc diameter and the floc size distribution at flocculation time of 6 min at different cationic polymer concentration. The arithmetic mean floc diameter d_{am} was computed from the floc size distribution data as [9]

$$d_{am} = \sum_i \bar{d}_i \upsilon_i \quad (21)$$

where $\bar{d}_i$ is arithmetic mean diameter of flocs in size class i and υ_i is floc volume fraction in the same size class. It can be seen from both Figs. 6 and 7 that the simulation results follow the experimental trend closely. As shown in Fig. 7, the model predicts narrower floc size distribution with the peaks rested at a higher volume fraction compared to the measured data. This could be due to the choice of the number of size classes and choosing a finer number of size classes could conceivably result in a more accurate computation of the floc size distribution data. However, this approach will be computationally more intensive which required long computational time and sometimes can lead to inaccurate solutions. Thus, there is a trade-off between solution accuracy and computational demand.

One of the important observations from Fig. 6 is that the flocs grow rapidly from its initial particle diameter of 64.2 μm to larger flocs in just within 3 min. After 3 min, the mean floc diameter remained constant until the end of flocculation time of 6 min. These observation shows that flocs breakage was minimal though it was a shear-induced flocculation at constant stirring of 200 rpm and the flocculation of POME in the presence of cationic polymer occurs by charge neutralization and bridging attraction. Bridging is often used in conjunction with charge neutralization to produce shear resistant flocs and their action was fast. At the same time, the flocs grow at larger mean floc diameter with increasing fractal dimension as the cationic polymer dosage increased. Fig. 7 shows that at flocculation time of 6 min, the produced peak of floc size distribution shift gradually from smaller floc size to larger floc size as the cationic polymer dosage increased. This confirmed that at higher dosage of cationic polymer, denser and larger flocs were produced and thus effective flocculation was obtained. However, cationic polymer dosage higher than 300 mg/L was not favorable in the present

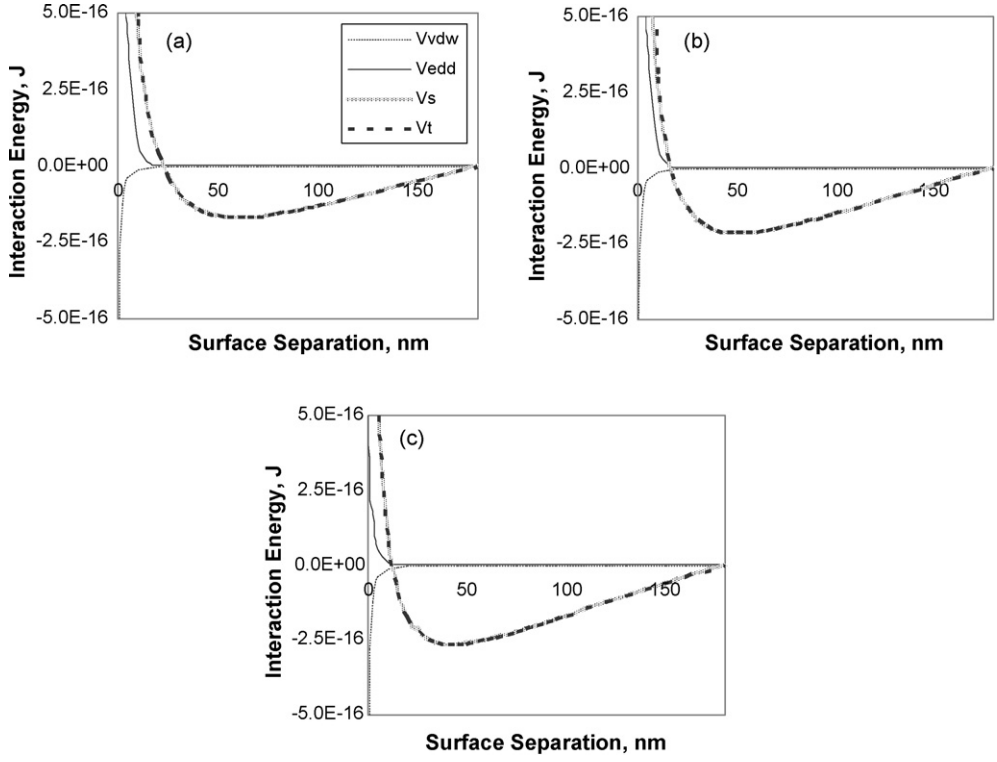

Fig. 10. The interaction energy curves for particles/flocs with adsorbed cationic–anionic polymer layers at cationic polymer dosage of 300 mg/L and anionic polymer dosage of (a) 10 mg/L with Γ/Γ_0 0.700, ψ_0 12.1 mV; (b) 30 mg/L with Γ/Γ_0 0.725, ψ_0 11.7 mV; (c) 50 mg/L with Γ/Γ_0 0.750, ψ_o −4.4 mV. V_{vdw} is van der Waals attraction, V_{edd} is electrical double layer repulsion, V_s is bridging attraction and V_t is the net interaction energy.

Table 4
Model parameters used in PBM for anionic polymer

Parameter	Value
Hamaker constant of the polyacrylic acid across a vacuum, A_s	8.0×10^{-20} J*
Polymer volume fraction at a single saturated surface, Φ_{So}	0.15
Adsorbed polymer layer thickness, δ	90 nm
Fractional polymer surface coverage, Γ/Γ_0	0.70–0.75
Surface potentials, ψ_{0i}	−4.4–12.1 mV

*Data from Vincent [21].

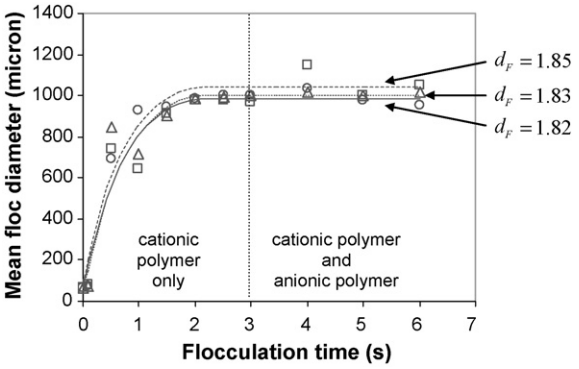

Fig. 11. Comparison of simulated and experimental time evolution of mean floc diameter with 300 mg/L cationic polymer and different anionic polymer dosage. Experimental: (◊) 10 mg/L, (△) 30 mg/L, (□) 50 mg/L and simulation: (——) 10 mg/L, (. . .) 30 mg/L, (—) −50 mg/L.

study due to the economic constraint as the polymer cost per unit is quite expensive.

The comparison of simulation results of suspended solids, COD, oil and grease concentration in pretreated POME by using the correlation of Eqs. (16)–(20) with the experimental results based on the average values taken from flocculation time of 3–6 min are shown in Fig. 8. Nevertheless, the simulation results follow the experimental trend closely. Thus, the correlation of indirect indicators (suspended solids, COD, oil and grease) with the floc size distribution based on the PBM has been successfully applied. Fig. 8 shows that the suspended solids, COD, oil and grease concentration of pretreated POME decrease as the cationic polymer dosage increases. Table 3 shows that the percent of suspended solids, COD, oil and grease removal increased as the fractal dimension and cationic polymer dosage increased. This implies that at higher cationic polymer dosage, more suspended solids were captured to produce larger and denser flocs and thus the suspended solids concentration in the pretreated POME was greatly reduced. Once the suspended solids concentration was reduced, the COD, oil and grease concentration of pretreated POME was also reduced.

As shown in Table 3, it is interesting to note that the percent of water recovery increased as the fractal dimension and cationic polymer dosage increased. The percent of water recovery is closely related to the flocs characteristic in a flocculation system, whereas the flocs characteristic is closely related to the fractal dimension. The dense flocs of high fractal dimension give high water recovery as less water is captured inside the dense flocs. It can be seen from Fig. 9, higher cationic polymer dosage resulted in higher net interaction energy which was attractive due to bridging attraction. At higher attraction energy, the particles were bridged in a more compact and intact manner to produce denser and large flocs with high fractal dimension.

Based on the results presented, the pretreated POME suspended solids concentration of below 100 mg/L is obtained at the cationic polymer dosage of 300 mg/L. The suspended solids concentration which exceeds 100 mg/L will cause serious fouling in the membrane separation. Thus, the cationic polymer dosage of 300 mg/L is chosen as the optimum dosage. Though at this dosage, the highest percent of water recovery (55.65%) was achieved, the efficiency of water recovery did not meet the target in the present investigation. At least 75% of water recovery was targeted to prevent large amount of water loss to the sludge and thus addition of anionic polymer (dual polymer system) is investigated in the following section to analyze the possibility of higher water recovery.

4.2. Dual polymer system

For the dual polymer system, the direct flocculation of POME was investigated by first adding the medium charge density with high molecular weigh cationic polymer (Polyfloc KP 9650) at the dosage of 300 mg/L under constant shear of 200 rpm. After stirring for 3 min, the high charge density with high molecular weigh anionic polymer (Polyfloc AP8350) was added under constant shear of 150 rpm. The raw POME was flocculated at its initial pH (without pH adjustment) and the floc distribution data, pretreated POME suspended solid, COD, oil and grease were obtained for each reaction time of 1–6 min.

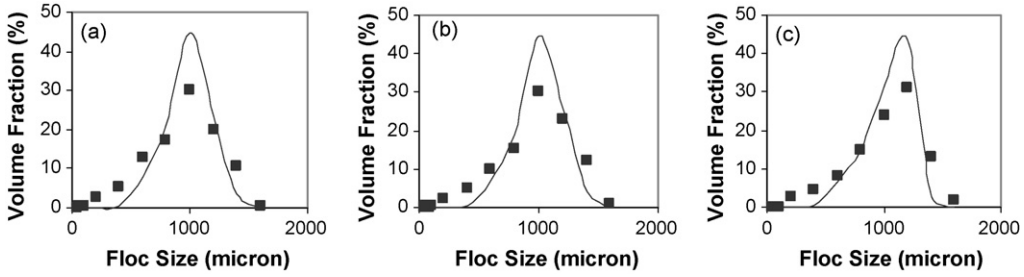

Fig. 12. Comparison of simulated and experimental floc size distribution obtained after 6 min of flocculation using 300 mg/L cationic polymer followed by (a) 10 mg/L; (b) 30 mg/L; (c) 50 mg/L anionic polymer. The solid lines are the simulation results while the dotted points are the experimental results.

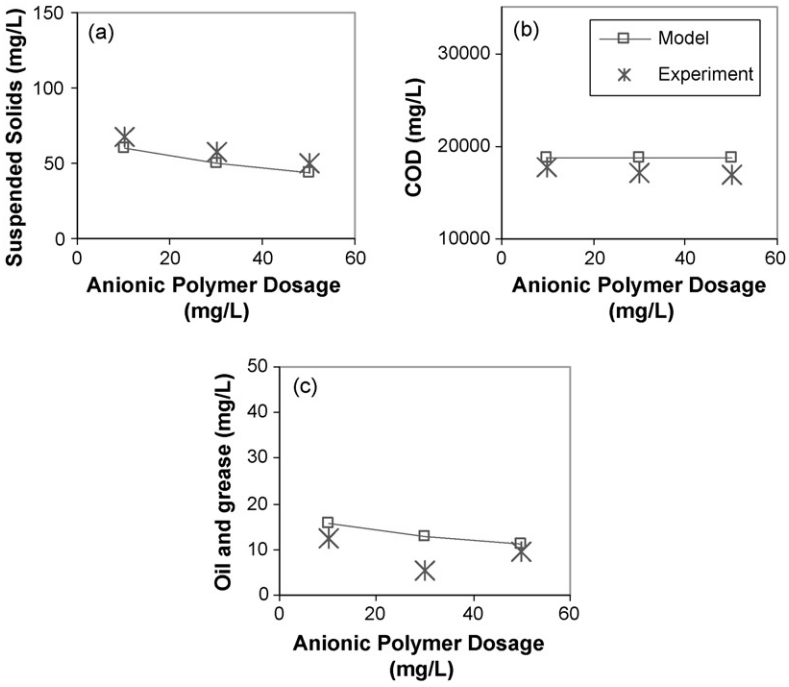

Fig. 13. Effect of anionic polymer dosage on (a) suspended solids; (b) COD; (c) oil and grease concentration of pretreated POME.

The PBM of Eq. (2) was solved and implemented in a similar manner as presented in the pervious section. At the flocculation time of 0–3 min, the model parameters follow the parameters of cationic polymer in Table 2. At the flocculation time of 3–6 min after the anionic polymer addition, the PBM was implemented by using the identical model parameters of cationic polymer except those presented in Table 4. In order to check the validity of the model parameters, interaction energies of Fig. 10 for each system of different anionic polymer dosage (10, 30, 50 mg/L) were computed between two polymer-coated particles/flocs. The particles/flocs are assumed coated with two layers of adsorbed polymers where the inner layer is the adsorbed cationic polymer and the outer layer is the adsorbed anionic polymer. As it can be seen from Fig. 10, the net interaction energy is always attractive following exactly the trend of bridging attraction. Thus, charge neutralization by anionic polymer is negligible and the bridging attraction is dominating. The negative charge of anionic polymer is not significant in this case because most of the small particles have already been captured as flocs by the cationic polymer.

The simulation results of dual polymer system using PBM based on the model parameters of Table 3 are compared in Figs. 11 and 12 with experimental results for time evolution of mean floc diameter and the floc size distribution at flocculation time of 6 min for different anionic polymer concentration. The arithmetic mean floc diameter, d_{am} was computed from the floc size distribution data using Eq. (21). Observation from both Figs. 11 and 12, the simulation results followed closely the experimental trend. Similar to the single polymer system of Fig. 7, Fig. 12 shows that the model predicts narrower floc size distribution with the peaks rested at a higher volume fraction compared to the measured data.

As shown from Fig. 11, at the initial flocculation (0–3 min), the flocs grow rapidly from its initial particle diameter of 64.2 μm to larger flocs due to the presence of 300 mg/L of cationic polymer. At the flocculation time of 3 min, anionic polymer was added and the flocculation was allowed to proceed to 6 min. However, the addition of anionic polymer does not induce significant flocs growth although the fractal dimension increased slightly from 1.82 to1.85 as the anionic polymer dosage increased. The final mean floc diameter obtained at the flocculation time of 6 min was approximately 1000 μm which was close to the value obtained from Fig. 6 where only 300 mg/L cationic polymer was used. Similarly, Fig. 12 shows that at flocculation time of 6 min, the peak of floc size distribution was obtained at approximately 1000 μm and the peaks shift only slightly from smaller floc size to larger floc size as the anionic polymer dosage increased. Besides, the observation of Figs. 11 and 12 shows that the flocs breakage was minimal though it was a shear-induced flocculation at constant stirring (200 rpm for 0–3 min and followed by 150 rpm for 3–6 min) as the mean floc diameter did not reduce at the end of flocculation. The flocs breakage was prevented by the bridging attraction of both cationic and anionic polymers by producing dense and shear resistant flocs.

Fig. 13 shows the comparison of simulation results of suspended solids, COD, oil and grease concentration in pretreated POME by using the correlation of Eqs. (16)–(20) with the experimental results based on the average values taken after the anionic polymer were added. The simulation results followed the experimental trend closely and the correlation of indirect indicators (suspended solids, COD, oil and grease) with the floc size distribution based on the PBM was successfully applied in the dual polymer system. Fig. 13 indicates that the suspended

solids concentration of pretreated POME decreased slightly as the anionic polymer dosage increased. As the suspended solids concentration reduction is minimal, the COD, oil and grease concentration of pretreated POME remain almost constant at increasing anionic polymer dosage. In correspond to Table 3, the percent of suspended solids, COD, oil and grease removal increases very slightly (almost constant) as the fractal dimension and anionic polymer dosage increase. In addition, there is no significant improvement of suspended solids, COD, oil and grease removal by using additional anionic polymer compared to the flocculation by using only 300 mg/L of cationic polymer.

Although additional of anionic polymer did not give significant effect on flocs growth, suspended solids, COD, oil and grease removal, the percent of water recovery increased tremendously as the fractal dimension and anionic polymer dosage increased as shown in Table 3. At the anionic polymer dosage of 50 mg/L, 80.78% of water recovery was obtained which was higher than the targeted water recovery of 75%. This shows that additional of anionic polymer produced dense flocs of high fractal dimension which gave high water recovery as less water was captured inside the flocs. Fig. 14 shows that additional of anionic polymer into the flocculation of POME significantly increased the net interaction energy of which was attractive by one order of magnitude compared to flocculation by using only 300 mg/L cationic polymer. It is also noted that higher anionic polymer dosage resulted in higher net interaction energy due to bridging attraction. This observation shows that though additional of anionic polymer did not give significant increase in flocs size, suspended solids, COD, oil and grease removal, the additional of anionic polymer increased the percent of water recovery by bridging those initially loose flocs to produce compact and dense flocs of higher fractal dimension.

In order to obtain the best flocculation results, the flocculation should be done by first adding 300 mg/L of cationic polymer at stirring of 200 rpm for 3 min. This is followed by adding 50 mg/L of anionic polymer at stirring of 150 rpm for 1 min to ensure homogenous mixing. Additional of anionic polymer in the POME flocculation system is important as high water recovery of at least 75% will ensure smooth operation of dewatering system besides preventing huge water loss to the sludge.

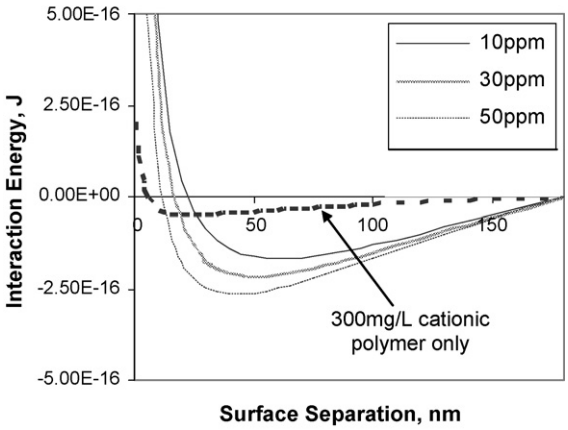

Fig. 14. Comparison between the net interaction energy curves of flocculation using 300 mg/L cationic polymer with the addition of anionic polymer at different dosage.

4.3. Preliminary cost analysis

A preliminary cost analysis presented in Table 5 was carried out to evaluate and compare the treatment costs between the direct flocculation of POME in the present study and the conventional coagulation–flocculation process presented in the literature (Ahmad et al. [1–2]). The cost estimates were based on the current market price in Malaysia, for all the materials

Table 5
Comparison of the treatment costs between the direct flocculation of POME and the conventional coagulation–flocculation process

Parameters	Direct flocculation	Conventional pretreatment*
1st stage		
Type of coagulant/flocculent	Cationic polymer	Alum
Dosage of coagulant/flocculent	300 mg/L POME treated	15 000 mg/L POME-treated
Unit cost of coagulant/flocculent	RM 15.50/kg	RM 1.00/kg
Total cost of coagulant/flocculent	RM 4.65/m^3 POME treated	RM 15.00/m^3 POME-treated
2nd stage		
pH adjustment	Not needed	Needed
3rd stage		
Type of flocculent	Anionic polymer	Cationic polymer
Dosage of flocculent	50 mg/L POME treated	300 mg/L POME-treated
Unit cost of flocculent	RM 9.00/kg	RM 11.00/kg
Total cost of flocculent	RM 0.45/m^3 POME treated	RM 3.30/m^3 POME-treated
Total treatment cost	RM 5.10/m^3 POME treated	RM 18.30/m^3 POME-treated
Suspended solids removal	99.66%	>99%
COD removal	55.79%	>50%
Oil and grease removal	99.66%	>99%
Water recovery	80.78%	78%

*The literature data obtained from A.L. Ahmad et al. [1–2]. Note: the current exchange rate of Malaysian Ringgit is 1USD = 3.48 RM (as at 22 August 2007).

as quoted by suppliers. Based on the comparison of treatment efficiency between direct flocculation and conventional pretreatment of POME in terms of water recovery, suspended solids, COD, oil and grease removal, the direct flocculation shows comparable treatment efficiency if it is not better. However, without even considering the cost of chemical used in pH adjustment for the conventional pretreatment, the total treatment cost of conventional pretreatment is 3.6 times higher than the total treatment cost of direct flocculation. Thus, the present study proves that direct flocculation is more cost effective than the conventional pretreatment of POME.

5. Conclusions

The present study has successfully investigated the efficiency of POME pretreatment by direct flocculation using the PBM. The proposed model has considered the charge neutralization and bridging attraction under shear-induced flocculation and the model predictions were found to reflect experimentally results adequately. The correlation of indirect indicators (suspended solids, COD, oil and grease) with the floc size distribution based on the PBM has also been successfully applied.

In the single polymer system, the cationic polymer was found to serve as double acting polymer by first neutralizing the negative charge of the particles (charge neutralization) and then flocs formation by bridging based on the interaction energy curves computed from the PBM. The optimum cationic polymer dosage was obtained as 300 mg/L at stirring of 200 rpm for 3 min to give 99.60%, 53.68%, 99.60% and 55.65% of suspended solids, COD, oil and grease removal, water recovery, respectively. The flocs breakage was minimal with the fractal dimension of 1.82 but the percent of water recovery was still low compared to the targeted water recovery of at least 75%.

In the dual polymer system, the additional of anionic polymer was found to serve as the bridging polymer based on the interaction energy curves computed from the PBM. The optimum anionic polymer dosage was obtained as 50 mg/L at stirring of 150 rpm for 1 min to give 99.66%, 55.79%, 99.66% and 80.78% of suspended solids, COD, oil and grease removal, water recovery, respectively. High water recovery was achieved as the anionic polymer bridged those initially loose flocs to produce compact, dense and shear resistant flocs of higher fractal dimension (1.85).

The proposed treatment of direct flocculation significantly reduced the treatment cost by a factor of 3.6 compared to the conventional coagulation–flocculation process with comparable treatment efficiency. Thus, the present study has shown that the inorganic coagulant could be completely replaced with water-soluble organic polymers in POME pretreatment by using direct flocculation without the need of pH adjustment under applied shear.

Acknowledgements

The authors would like to gratefully acknowledge Federal Land Development Authority Foundation (Yayasan Felda) of Malaysia, for their financial support. The authors would also like to thank United Oil Palm Industry, Nibong Tebal, Pulau Pinang, for providing the sample of POME to conduct this research.

References

[1] A.L. Ahmad, S. Ismail, S. Bhatia, Water recycling from palm oil mill effluent (POME) using membrane technology, Desalination 157 (2003) 87–95.
[2] A.L. Ahmad, S. Ismail, S. Bhatia, Optimization of coagulation–flocculation process for palm oil mill effluent using response surface methodology, Environ. Sci. Technol. 39 (2005) 2828–2834.
[3] A. Vilgé-Ritter, A. Masion, T. Boulangé, D. Rybacki, J.Y. Bottero, Removal of natural organic matter by coagulation–flocculation: a pyrolysis–GC–MS Study, Environ. Sci. Technol. 33 (1999) 3027–3032.
[4] D. Wang, H. Tang, J. Gregory, Coagulation behavior of aluminum salts in eutrophic water: significance of Al_{13} species and pH control, Environ. Sci. Technol. 40 (2006) 325–331.
[5] J.D. Lee, S.H. Lee, M.H. Jo, P.K. Park, C.H. Lee, J.W. Kwak, Effect of coagulation conditions on membrane filtration characteristics in coagulation–microfiltration process for water treatment, Environ. Sci. Technol. 34 (2000) 3780–3788.
[6] R. Sarika, N. Kalogerakis, D. Mantzavinos, Treatment of olive mill effluents. Part II. Complete removal of solids by direct flocculation with poly-electrolytes, Environ. Int. 31 (2005) 297–304.
[7] L. Ravina, Everything You Want to Know About Coagulation and Flocculation, 4th ed., Zeta-Meter, Inc., USA, 1993, p. 13.
[8] P. Somasundaran, V. Runkana, Modeling flocculation of colloidal mineral suspensions using population balances, Int. J. Miner. Process. 72 (2003) 33–55.
[9] V. Runkana, P. Somasundaran, P.C. Kapur, A population balance model for flocculation of colloidal suspensions by polymer bridging, Chem. Eng. Sci. 61 (2006) 182–191.
[10] V. Runkana, P. Somasundaran, P.C. Kapur, Mathematical modeling of polymer-induced flocculation by charge neutralization, J. Colloid Interface Sci. 270 (2004) 347–358.
[11] A. Ding, M.J. Hounslow, C.A. Biggs, Population balance modeling of activated sludge flocculation: Investigating the size dependence of aggregation, breakage and collision efficiency, Chem. Eng. Sci. 61 (2006) 63–74.
[12] N.K. Nere, D. Ramkrishna, Solution of population balance equation with pure aggregation in a fully developed turbulent pipe flow, Chem. Eng. Sci. 61 (2006) 96–103.
[13] A. Gerstlauer, C. Gahn, H. Zhou, M. Rauls, M. Schreiber, Application of population balances in the chemical industry—current status and future needs, Chem. Eng. Sci. 61 (2006) 205–217.
[14] M. Smoluchowski, Drei vortrage uber diffusion, Brownsche molekularbewegung und koagulation vor kolloidteilchen, Physikalische Zeitschrift 17 (1916) 557–571.
[15] S. Kumar, D. Ramkrishna, On the solution of population balance equations by discretization: I. A fixed pivot technique, Chem. Eng. Sci. 51 (1996) 1311–1332.
[16] P.T. Spicer, S.E. Pratsinis, Coagulation and fragmentation: universal steady-state particle size distribution, AIChE J. 42 (1996) 1612–1620.
[17] A. Thill, S. Moustier, J. Aziz, M.R. Wiesner, J.Y. Bottero, Flocs restructuring during aggregation: experimental evidence and numerical simulation, J. Colloid Interface Sci. 243 (2001) 171–182.
[18] G.C. Bushell, Y.D. Yan, D. Woodfield, J. Raper, R. Amal, On techniques for the measurement of the mass fractal dimension of aggregates, Adv. Colloid Interface Sci. 95 (2002) 1–50.
[19] D.C. Hopkins, J.J. Ducoste, Characterizing flocculation under heterogeneous turbulence, J. Colloid Interface Sci. 264 (2003) 184–194.
[20] J.C. Flesch, P.T. Spicer, S.E. Pratsinis, Laminar and turbulence shear-induced flocculation of fractal aggregates, AIChE J. 45 (1999) 1114–1124.
[21] B. Vincent, The van der Waals attraction between colloid particles having adsorbed layers II. Calculation of interaction curves, J. Colloid Interface Sci. 42 (1973) 270–285.
[22] M.J. Vold, The effect of adsorption on the van der Waals interaction of spherical colloidal particles, J. Colloid Sci. 16 (1961) 1–12.

[23] J. Gregory, Approximate expressions for retarded van der Waals interaction, J. Colloid Interface Sci. (1981) 138–145.
[24] G.M. Bell, S. Levine, L.N. McCartney, Approximate methods of determining the double-layer free energy of interaction between two charged colloidal spheres, J. Colloid Interface Sci. 33 (1970) 335–359.
[25] J.N. Israelachvili, Intermolecular and Surface Forces, 2nd ed., Academic Press, New York, 1991.
[26] P.G. de Genes, Polymer solutions near an interface. 1. Adsorption and depletion layers, Macromolecules 14 (1981) 1637–1644.
[27] P.G. de Genes, Polymer solutions near an interface. 2. Interaction between two plates carrying adsorbed polymer layers, Macromolecules 15 (1982) 492–500.
[28] A. Flesh, Laminar and turbulent shear-induced flocculation of fractal aggregate, AIChE J. 45 (1999) 1114–1124.
[29] M.C. Sterling Jr., J.S. Bonner, A.N.S. Ernest, C.A. Page, R.L. Autenrieth, Application of fractal flocculation and vertical transport model to aquatic sol–sediment systems, Water Res. 39 (2005) 1818–1830.
[30] R. Amal, J.R. Coury, J.A. Raper, W.P. Walsh, T.D. Waite, Structure and kinetics of aggregating colloidal hematite, Colloids Surf. A46 (1990) 1–19.
[31] American Public Health Association, Standard Methods for the Examination of Water and Wastewater, APHA, Washington, DC, 1999.
[32] C. Selumulya, G. Bushell, R. Amal, T.D. Waite, Aggregate properties in relation to aggregate conditions under various applied environments, Int. J. Miner. Process. 73 (2004) 295–307.
[33] D.N. Thomas, S.J. Judd, N. Fawcett, Flocculation modeling: a review, Water Res. 33 (1999) 1579–1592.
[34] A. Constantinides, N. Mostoufi, Numerical Methods for Chemical Engineers with MATLAB Applications, Prentice Hall PTR, New Jersey, 1999.
[35] J. Klein, G. Rossi, Analysis of the experimental implications of the scaling theory of polymer adsorption, Macromolecules 31 (1998) 1979–1988.
[36] T. Cosgrove, T.L. Crowley, K. Ryan, J.R.P. Webster, The effects of solvency on the structure of an adsorbed polymer layer and dispersion stability, Colloids Surf. A51 (1990) 255–269.
[37] C.J. Van Oss, Interfacial Forces in Aqueous Media, Marcel Dekker, New York, 1994.